Syntheses, Spectro-Electrochemical Studies, and Molecular and Electronic Structures of Ferrocenyl Ene-diynes

ARTICLE *in* ORGANOMETALLICS · OCTOBER 2013

Impact Factor: 4.13 · DOI: 10.1021/om400535y

8 AUTHORS, INCLUDING:

Qiang Zeng
South China University of Technology
24 PUBLICATIONS **125** CITATIONS
SEE PROFILE

Matthias Parthey
Technische Universität Berlin
10 PUBLICATIONS **117** CITATIONS
SEE PROFILE

František Hartl
University of Reading
165 PUBLICATIONS **3,367** CITATIONS
SEE PROFILE

Paul J. Low
University of Western Australia
209 PUBLICATIONS **4,255** CITATIONS
SEE PROFILE

ORGANOMETALLICS

Article

pubs.acs.org/Organometallics

Syntheses, Spectroelectrochemical Studies, and Molecular and Electronic Structures of Ferrocenyl Ene-diynes

Kevin B. Vincent,[†] Qiang Zeng,[‡] Matthias Parthey,[§] Dmitry S. Yufit,[†] Judith A.K. Howard,[†] František Hartl,*[,‡] Martin Kaupp,*[,§] and Paul J. Low*[,†,∥]

[†]Department of Chemistry, Durham University, South Road, Durham DH1 3LE, U.K.

[‡]Department of Chemistry, University of Reading, Whiteknights, Reading RG6 6AD, U.K.

[§]Technische Universität Berlin, Institut für Chemie, Sekr. C7, Strasse des 17. Juni 135, 10623 Berlin, Germany

[∥]School of Chemistry and Biochemistry, University of Western Australia, 35 Stirling Highway, Crawley, Perth 6009, Australia

Supporting Information

ABSTRACT: The readily available complex 1,1-dibromo-2-ferrocenylethylene provides a convenient entry point for the preparation of a wide range of cross-conjugated 1,1-bis(alkynyl)-2-ferrocenylethenes through simple Pd(0)/Cu(I)-mediated cross-coupling reactions with 1-alkynes. The ferrocene moiety in compounds of the general form $FcCH{=}C(C{\equiv}CR)_2$ is essentially electronically isolated from the cross-conjugated π system, as evidenced by IR and UV−vis spectroelectrochemical experiments and quantum chemical calculations. In contrast to the other examples which give stable ferrocenium derivatives upon electrochemical oxidation, the aniline derivatives $[FcCH{=}C(C{\equiv}CC_6H_4NH_2\text{-}4)_2]^+$ and $[FcCH{=}C(C{\equiv}CC_6H_4NMe_2\text{-}4)_2]^+$ proved to be unstable on the time scale of the spectroelectrochemical experiments, leading to passivation of the electrode surface over time. There is no significant thermodynamic stabilization of the radical anion $[FcCH{=}C(C{\equiv}CC_6H_4NO_2\text{-}4)_2]^-$ relative to the neutral and dianionic analogues, although the dianion $[FcCH{=}C(C{\equiv}CC_6H_4NO_2\text{-}4)_2]^{2-}$ could be studied as a relatively chemically stable species and is well described in terms of two linked nitrophenyl radicals. The capacity to introduce a relatively isolated point charge at the periphery of the cross-conjugated π system appears to make these complexes useful templates for the construction of electrochemically gated quantum interference transistors.

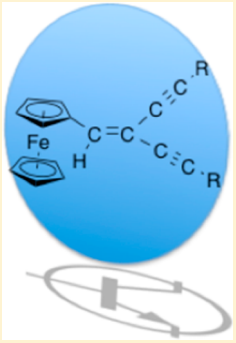

INTRODUCTION

Redox-active moieties linked by linear conjugated π systems, and the mixed-valence complexes that can be generated following one-electron redox processes, have been topics of immense interest for many decades.[1] Such "$[L_xM_A]$−bridge−$[M_BL_x]$" systems provide incentives for the development of synthetic methods, such as those used in the preparation of long linear polyynediyl chains stabilized by end-capping metal complexes $[L_xM]\{\mu\text{-}(C{\equiv}C)_n\}[ML_x]$,[2] and explorations of electronic structure through studies of intramolecular electron-exchange processes mediated by the linear all-carbon bridge.[3−7] Cross-conjugated structures are also attracting attention driven by similar ambitions,[8] with the unique geometric properties of the prototypical diethynylethene fragment leading to its incorporation into a range of shape-persistent macrocycles,[9] radiannulene derivatives,[10] and tetraethynyleneethenes.[11] Together, these families of cross-conjugated compounds comprise a series of materials with useful electronic and optical properties that complement those of the related linearly conjugated analogues.[12] In addition, cross-conjugated fragments are now being recognized as potential scaffolds through which to explore the influence of quantum interference effects on the promotion and mediation of trans-molecule conductance in molecules and nascent molecular electronic devices.[13] In turn, this has led to a growing number of studies in which cross-conjugated carbon-rich ligands are being incorporated into metal complexes[14] and attracting interest in the potential for intramolecular electron transfer between metal centers through the cross-conjugated bridge.[15]

Against this background of fundamental and applied research interests, it is unsurprising to note that perhaps the most ubiquitous of all redox probes, ferrocene, has been incorporated into a wide range of cross-conjugated molecules (e.g., **A**−**G**; Chart 1).[16] In this report we describe convenient synthetic routes to 1,1-bis(alkynyl)-2-ferrocenylethene derivatives (**A**) from the readily available precursor 1,1-dibromo-2-ferrocenylethylene. (Spectro)electrochemical characterization and supporting quantum chemical calculations are used to explore the interactions between the ferrocenyl moiety and the cross-conjugated ancillary group, and the results are considered briefly against a recently proposed molecular structure for a chemically or electrochemically gated, quantum-interference-based molecular transistor.

Special Issue: Ferrocene - Beauty and Function

Received: June 10, 2013
Published: August 9, 2013

   dx.doi.org/10.1021/om400535y | *Organometallics* 2013, 32, 6022−6032

Chart 1. Selection of Representative Ferrocene-Containing Cross-Conjugated Compounds[16]

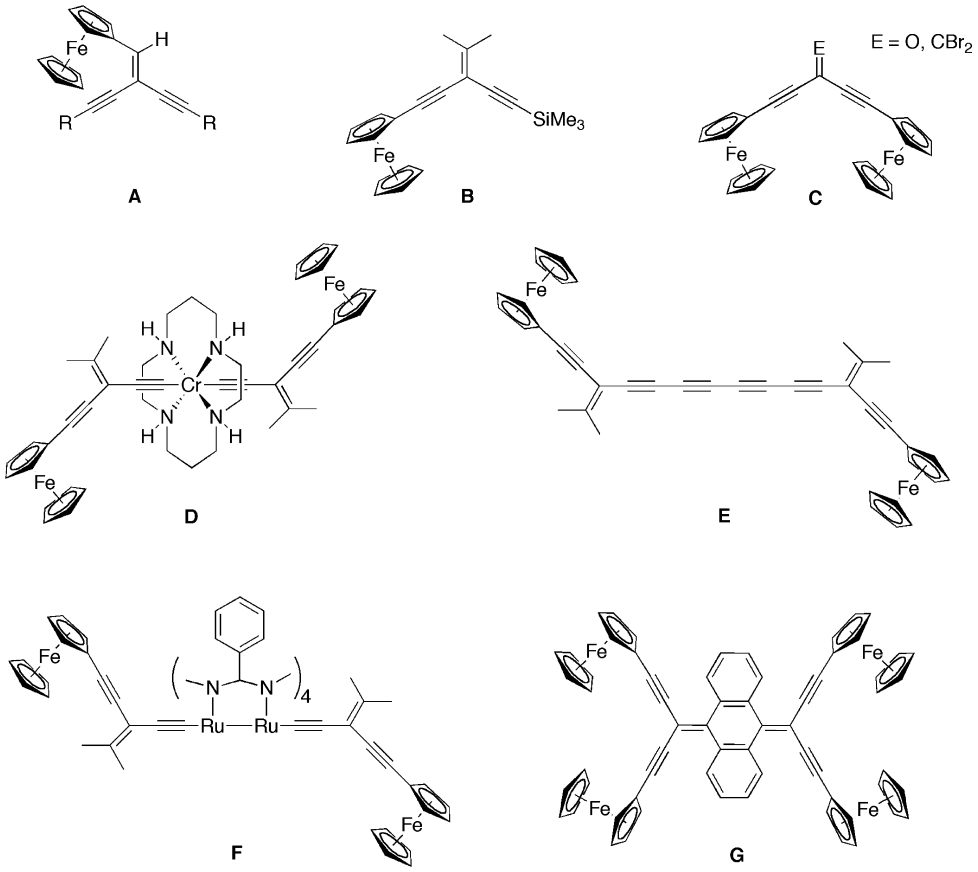

Scheme 1. Preparation of Compounds 2 and 3a–f from 1 via 5a–e

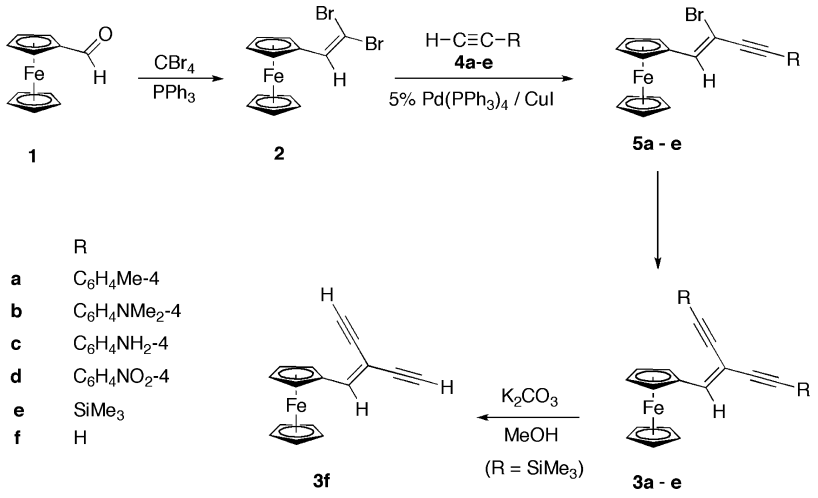

RESULTS AND DISCUSSION

Syntheses and Characterization. The key precursor 1,1-dibromo-2-ferrocenylethene (**2**) is readily prepared from the reaction of ferrocenecarboxaldehyde (Fc-CHO, **1**) with PPh_3/CBr_4 (Corey–Fuchs reaction) (Scheme 1).[17,18] Compound **2** is a versatile precursor of ethynylferrocene,[18,19] but despite the wider synthetic versatility of 1,1-dihalovinyl compounds,[12h,20] other reactions of **2** appear to be limited to the preparation of ferrocene-substituted vinylic dithioethers and heterometallic oxidative addition products.[21]

One appealing aspect of the chemistry of 1,2- and 1,1-dihalovinyl compounds is their facility to enter into Pd(0)/Cu(I)-catalyzed cross-coupling reactions with terminal alkynes to give a range of linear[22] and cross-conjugated[11e,h,23] ene-(mono-, di-, or tetra)ynes. The recent description of a chemically gated quantum-interference-based molecular transistor architecture based on a 1,1-diethynylethene (Figure 1) prompts renewed consideration of such structures.[13] In the model put forward by Grozema, a donor D (or source electrode) is connected to an acceptor, A (or drain electrode), via a cross-conjugated bridge. The gating component, G, is

dx.doi.org/10.1021/om400535y | Organometallics 2013, 32, 6022–6032

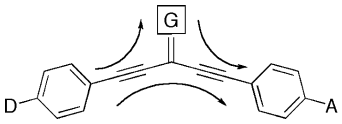

Figure 1. Schematic of the Grozema molecular transistor. The arrows show the propagation of the components of the wave function directly between donor, D, and acceptor, A, and also the portion traveling via the gate, G. The moieties D and A may be distinct chemical groups or the source and drain electrodes of a device.

chosen to be capable of changing charge state through chemical or electrochemical means. The cross-conjugated structure limits charge flow from D to A as the components of the charge carrier wave function propagating directly from D to A and that traveling via the channel to the gate G interact and form an interference pattern. This interference can be constructive or destructive, depending on the chemical structure of the side chain; in the case of the structure shown in Figure 1, interference will be destructive and the transistor will be normally off. Chemical modification of the charge on the gating moiety (G) by (de)protonation or metal-ion binding to groups along the gate pathway changes the energy of the path and under favorable conditions will prevent a fully destructive interference pattern from being formed, hence increasing the flow of charge from D to A. Redox-active gate groups were also noted as providing a suitable means for switching these interference effects. With these points in mind, cross-coupling reactions of **2** with terminal alkynes to generate the prototypical structures **A** (Chart 1) in which the ferrocene moiety can serve as an electrochemically addressable means of introducing a point charge to gate the flow of charge were investigated.

Reaction of **2** with a large excess of terminal alkynes HC≡CC_6H_4R-4 (**4**: R = Me (**a**), NMe_2 (**b**), NH_2 (**c**), NO_2 (**d**)) or HC≡$CSiMe_3$ (**4e**) under Sonogashira cross-coupling conditions (NEt_3, $Pd(PPh_3)_4$/CuI) gave moderate to good yields of the desired 1,1-bis(alkynyl)-2-ferrocenylethenes **3a**−**e** (Scheme 1) as dark red solids (**3a**−**d**) or an oil (**3e**). While **4a**−**c** were chosen as representative electron-neutral, -donating and -withdrawing substituents, the amino (**4c**) and trimethylsilyl (**4e**) groups are potential surface binding groups.[24] Desilylation of **3e** by treatment with K_2CO_3/MeOH gave the fairly insoluble terminal dialkyne **3f** in good yield, which has potential for use as a reagent for the preparation of other derivatives featuring the 1,1-bis(alkynyl)-2-ferrocenylethene core.

The low chemoselectivity of 1,1-dibromoalkenes toward Sonogashira cross-coupling protocols has been noted previously,[23b,c] and in the present work attempts to selectively couple the less hindered vinyl bromide through reaction of **2** with 1 equiv of **4c**−**e** as representative alkynes gave a mixture of the appropriately substituted mono (**5**)- and dialkynylated (**3**) products and unreacted **2**. A survey of various coupling conditions, including the use of $PdCl_2$(dppf) as a catalyst precursor[23a] (dppf = 1,1′-bis(diphenylphosphino)ferrocene), failed to permit selective preparation of the monocoupled bromo ene-ynes **5** free of **2** and **3**. In the case of reaction with $PdCl_2(PPh_3)_2$ a much higher catalyst loading (ca. 20%) was required to achieve appreciable reaction yields of **3**, but no selectivity in the reaction toward products **5** was observed. However, from the reaction solution that yielded **3d** careful column chromatography permitted the isolation of a small amount of a second, higher polarity compound from a number of other ferrocene-containing byproducts, identified as *Z*-**5d** by single-crystal X-ray diffraction (vide infra). While this compound crystallized as the *Z* isomer (*Z*-**5d** vinylic proton δ_H 7.19 ppm), in solution the compound undergoes equilibration over the course of several hours to give an approximately 1:1 mixture of *E*- and *Z*-**5d**, as evidenced by the appearance and integration of a second set of vinylic and $C_6H_4NO_2$ proton resonances (*E*-**5d** vinylic proton δ_H 7.05 ppm and aromatic resonances at δ_H 7.76, 8.30 ppm).

Compounds **3a**−**g** were all characterized by the usual range of ^{1}H and ^{13}C{^{1}H} NMR spectroscopy (Figure 2), atmospheric

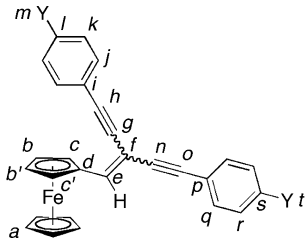

Figure 2. NMR labeling scheme for **3a**−**d**. Similar schemes for **3e**,**f** are given in the Supporting Information.

solids analysis probe (ASAP) mass spectrometry,[25] elemental analyses, and, in the case of **3d** and *Z*-**5d**, also by single-crystal X-ray diffraction. Each compound featured the expected pattern of ^{1}H resonances for a monosubstituted ferrocene. The equivalence of the $H_b/H_{b'}$ and $H_c/H_{c'}$ protons and the detection of a single cross peak from the $H_c/H_{c'}$ resonance to the vinylic proton (H_e) in the NOESY spectrum indicate that there is free rotation of the ferrocenyl moiety around the C_d−C_e bond. The two para-substituted aryl groups in **3a**−**d** gave rise to two pairs of resonances, reflecting the different dispositions across the double bond with respect to the ferrocenyl moiety, but individual pairs of resonances could not be unambiguously assigned to the *Z* or *E* branches of the ligand. The chemical shifts of the $H_c/H_{c'}$ and vinylic (H_e) protons and vinyl carbon resonances C_e (identified by HSQC spectroscopy and the coupling to the vinyl proton H_e) and C_f (identified by HMBC to H_e) were sensitive to the electronic character of the aryl substituent, and clearly there is some degree of electronic information being propagated through the cross-conjugated backbone. The trimethylsilyl-protected and terminal alkyne derivatives **3f**,**g** were similarly identified, with two $SiMe_3$ or ≡CH resonances observed, respectively. However, while the sets of resonances belonging to the individual alkynyl fragments were unambiguously assigned through a combination of ^{1}H−^{1}H and ^{1}H−^{13}C 2-D NMR experiments, as in the case of the phenylene protons, assigning these sets of ^{13}C resonances to either the *E* or the *Z* arm was not possible.

The IR spectra of **3a**−**e** were recorded in solution (CH_2Cl_2). Given the low solubility of **3f**, spectra were also obtained in the solid state (ATR-FTIR) for comparison, with the exception of the oil **3e**. The results are summarized in Table 1, and figures showing the ATR-FTIR spectra are given in the Supporting Information. All of these compounds display ν(C−H) bands associated with the cyclopentadienyl rings and, in the case of **3a**−**d**, the phenylene rings, in the region of 2750−3200 cm^{-1} which were more clearly observed in the solid-state spectra. For **3a**,**b**, this region also involves ν(C−H) bands from the terminal methyl groups. In the solid state a weak ν(C≡C) band is

dx.doi.org/10.1021/om400535y | *Organometallics* 2013, 32, 6022−6032

Table 1. Characteristic IR-Active Vibrational Modes (cm^{-1}) of 3a−e Observed in Solution (CH_2Cl_2 and $CH_2Cl_2/10^{-1}$ M Bu_4NPF_6) and the Solid State (ATR-FTIR), Spectroelectrochemical Data for $[3a-d]^{n+}$ (n = 0, 1), and Calculated Vibrational Frequencies for $[3a']^{n+}$, $[3b']^{n+}$, and $[3d']^{n+}$ (n = 0, 1)

	ν(N−H)	ν(C−H)	ν(C≡C)	ν(C=C) aryl	ν(C=C) vinyl	ν(C−N)	ν(NO_2)
3a[a]		3155−2800	2209, 2196	1607, 1509	1577		
3a[b]			2208, 2194	1609, 1510	1575		
[**3a**]$^{+}$[b]			2208, 2194	1605, 1510	1559		
3a′[c]			2233, 2220	1619, 1617, 1499, 1495	1585		
[**3a′**]$^{+}$[c]			2227, 2211	1615, 1556, 1499	1561		
3a[d]		3150, 2800	2200, 2176	1604, 1508	1564		
3b[a]		3150−2774	2205, 2186	1608, 1523	not obsd	1482, 1422, 1357	
3b[b]			2188	1607, 1522	not obsd		
[**3b**]$^{+}$[b]			2167	1605, 1524	1545		
3b′[c]			2223, 2210	1614, 1613, 1514, 1511			
[**3b′**]$^{+}$[c]			2203, 2178	1611, 1604, 1518, 1510	1527		
3b[d]		3100−2750	2189	1606, 1519	1576	1361	
3c[a]	3394[e]	3050−2800	2204−2190	1606, 1515	not obsd		
3c[b]	3395[e]		2185	1607, 1514	not obsd		
[**3c**]$^{+}$[b]	3400		2173	1603, 1517	1545		
3c[d]	3400[f]	3200−2800	2191	1605, 1514	1575	1296	
3d[a]		2830−3035	2195, 2210	1593, 1493	1565		1518, 1344
3d[b]			2211, 2195	1594, 1491	1565		1520, 1343
[**3d**]$^{+}$[b]			2215, 2201	1596, 1493	1565		1522, 1345
3d′[c]			2233, 2217	1601, 1566, 1482, 1478	1568, 1567		1636, 1634, 1395, 1393
[**3d′**]$^{+}$[c]			2237, 2223	1608, 1605, 1573, 1572, 1483, 1463	1576		1641, 1639, 1403, 1401
3d[d]		3150−2800	2188, 2211	1592, 1499	1561		1509, 1339
3e[a]		3050−2800	2144		1577		
3f[d]		3300,[g] 2775−3200	2100		1581		

[a] CH_2Cl_2 solution state. [b] $CH_2Cl_2/10^{-1}$ M Bu_4NPF_6. [c] Calculated, with 0.95 correction factor applied. [d] Solid state. [e] The corresponding bending vibration lies at 1622 cm^{-1} in pure CH_2Cl_2 and $CH_2Cl_2/10^{-1}$ M Bu_4NPF_6. [f] The corresponding bending vibration lies at 1619 cm^{-1}. [g] ν(C≡C−H).

observed around 2190 cm^{-1} for **3b**,**c**; the band pattern becomes more complex for **3a** and especially **3d**, while in solution the ν(C≡C) bands appeared as relatively sharp bands near 2190 cm^{-1} with a higher frequency shoulder in the case of the aryl derivatives, possibly reflecting Fermi coupling. The aryl and vinyl ν(C=C) wavenumbers are modestly sensitive to the electronic character of the substituent, with a small shift to lower energy in the case of the donor−acceptor deriative **3d** arguably reflecting a contribution from a more cumulated resonance form (Figure 3). In the donor (ferrocene)−donor (amine) derivatives **3b**,**c** the ν(C=C) vinyl bands were not observed in solution, likely due to the lack of a strong dipole. However, in the solid state, a band at 1575 (**3b**)/1576 cm^{-1} (**3c**) was clearly observed and likely gains intensity due to local distortions brought about by solid-state packing.

Single crystals of **3d** (Figure 4) and *Z*-**5d** (Figure 5) suitable for X-ray diffraction were obtained by slow diffusion of ethanol into solutions of the compound in CH_2Cl_2. Important bond lengths and angles are summarized in the relevant figure captions. As expected, the 1,1-dialkynylethene portions of the molecules are planar within 0.03 Å, and the key C=C (**3d**, 1.355(3) Å; *Z*-**5d**, 1.335(4) Å), =C−C (**3d**, 1.437(3), 1.434(3) Å; *Z*-**5d**, 1.422(4) Å), and C≡C (**3d**, 1.199(3), 1.197(3) Å; *Z*-**5d**, 1.190(4) Å) bond lengths are consistent across both compounds. The C(1)−C(5) ring of the vinylferrocene moiety also lies close to this plane, evidencing a degree of delocalization between the metal and cross-conjugated fragments. Interestingly, in the molecule **3d** the C(1)−C(5) ring and the aromatic group located *trans* across the double bond lie close to the same plane. The nitrophenyl groups *cis* to the vinylferrocene moiety are less obviously positioned to promote significant π conjugation. It should be

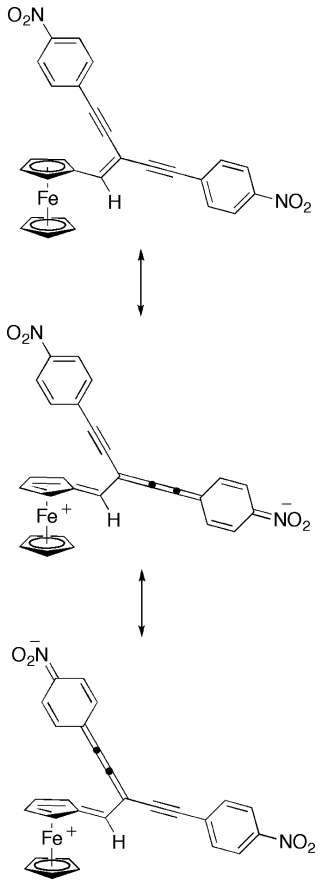

Figure 3. Resonance structures of the donor−acceptor compound **3d**.

dx.doi.org/10.1021/om400535y | *Organometallics* 2013, 32, 6022−6032

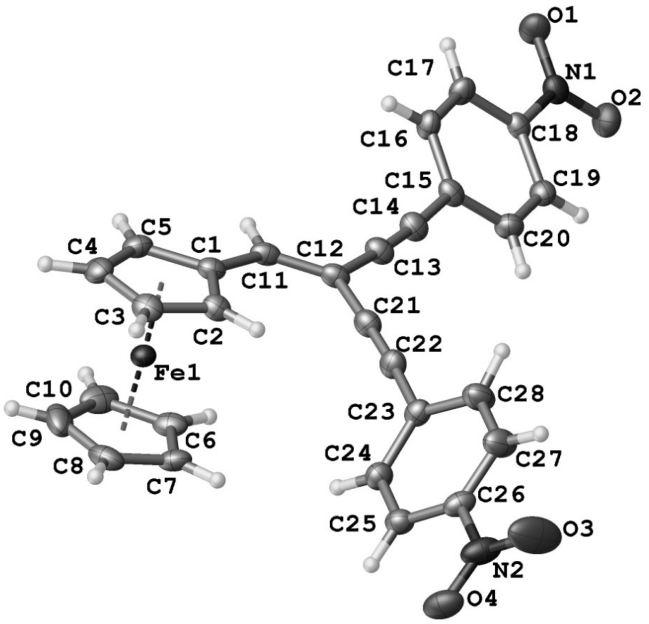

Figure 4. Plot of a molecule of **3d**, showing the atom-labeling scheme. Selected bond lengths (Å) and angles (deg): C1−C11 = 1.445(3), C11−C12 = 1.355(3), C12−C13 = 1.434(3), C13−C14 = 1.197(3), C14−C15 = 1.435(3), C12−C21 = 1.437(3), C21−C22 = 1.199(3), C22−C23 = 1.434(3); C1−C11−C12 = 129.8(2), C11−C12−C13 = 119.3(2), C11−C12−C21 = 123.4(2).

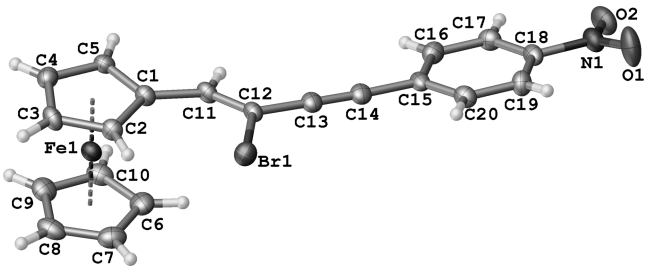

Figure 5. Plot of a molecule of **5d**, showing the atom-labeling scheme. Selected bond lengths (Å) and angles (deg): C1−C11 = 1.442(4), C11−C12 = 1.335(4), C12−C13 = 1.422(4), C13−C14 = 1.190(4), C14−C15 = 1.434(4); C1−C11−C12 = 132.6(3), C11−C12−C13 = 123.8(3).

noted that in the crystal of **3d** only the *trans*-nitrophenyl group takes part in $\pi\cdots\pi$ intermolecular interactions, while the *cis* group forms only various C−H$\cdots\pi$ and O$\cdots$CH short contacts.

Cyclic Voltammetry and Spectroelectrochemical Studies. The electrochemical response of the ferrocenyl compounds **3a−g** were investigated by cyclic voltammetry (CV) in a standard three-electrode cell (equipped with a Pt-microdisk working electrode) from a CH_2Cl_2 solution containing thesupporting electrolyte 10^{-1} M Bu_4NPF_6 . All potentials are reported against the ferrocene/ferrocenium (Fc/Fc^+) couple by reference to an internal decamethylferrocene (Fc^*) standard (−0.48 V vs Fc/Fc^+) (Table 2). The CV of each of the monoferrocenyl complexes **3a−f** displayed a reversible (or nearly so) one-electron anodic wave consistent with the redox properties of the ferrocenyl moiety. The electron-withdrawing nature of the conjugated vinyl group was evidenced in the shift of these waves to more positive potentials relative to ferrocene. In addition, across the series, the potentials were also sensitive to the electronic character of

Table 2. Oxidation Half-Wave Potentials for 3a−f[a]

compd	$E_{1/2}$/V
3a	0.18
3b	0.09
3c	0.10
3d[b]	0.22
3e	0.16
3f	0.19

[a]Conditions: $CH_2Cl_2/10^{-1}$ M Bu_4NPF_6; ν = 100 mV s^{-1}. Potentials are reported against ferrocene (Fc/Fc^+ = 0.0 V) by reference against an internal decamethylferrocene/decamethylferrocenium couple (Fc^*/Fc^{*+} = −0.48 V vs Fc/Fc^+). [b]Compound **3d** undergoes reversible reduction at $E_{1/2}$ = −1.42 V.

the remote substituent, with the electron-withdrawing $-NO_2$ group giving rise to the most positive potential shift (Table 2). The nitrophenyl groups in **3d** were also electroactive within the electrochemical window of the solvent, giving rise to two overlapping reduction waves (apparent $E_{1/2}$ = −1.42 V, ΔE_p = 100 mV) and the formation of $[\mathbf{3d}]^{2-}$. There was no evidence for any appreciable stability of the organic mixed-valence form $[\mathbf{3d}]^{-}$.

UV−vis−near-IR and IR spectroelectrochemical investigations were undertaken to better assess the interactions between the ferrocenyl moieties and the 1,1-dialkynylvinyl moiety in the most easily handled compounds **3a−d**. As **3d** exhibits both a reversible ferrocenyl-centered oxidation and a reduction localized on the terminal nitrophenyl substituents, it provides an ideal platform for spectroelectrochemical investigation of both the cathodic and anodic processes that will promote understanding of the electronic interactions between the redox sites and the 1,1-dialkynyl vinyl moiety. As shown in Figure 6,

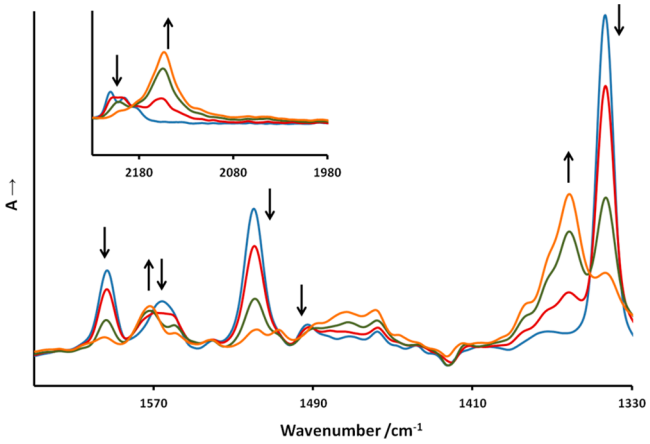

Figure 6. Reversible IR spectral changes accompanying reduction of the terminal nitrophenylene groups in **3d** in $CH_2Cl_2/10^{-1}$ M Bu_4NPF_6 within an OTTLE cell. The inset illustrates the ν(C≡C) region. The spectral changes between 1410 and 1490 cm^{-1} are caused by fluctuations of the electrolyte absorption.

the reduction of the nitro group induces a shift of the $\nu(NO_2)$ band at 1343 cm^{-1} to 1360 cm^{-1} and a decay of $\nu(NO_2)$ at 1520 cm^{-1}. Similar observations have been reported in comparisons of the IR spectra of nitrobenzene and its radical anion.[26] The $\nu(C{=}C)_{aryl}$ absorptions at 1491 and 1594 cm^{-1} are very weak in the reduced species, while the $\nu(C{=}C)_{vinyl}$ and $\nu(C{=}C)$ bands maintain the relatively high intensity (Table 1). The spectral changes reveal a very small shift of the

dx.doi.org/10.1021/om400535y | *Organometallics* 2013, 32, 6022−6032

ν(C═C)$_{vinyl}$ band at 1565 to 1570 cm^{-1} and a more significant low-energy shift of the ν(C≡C) absorption, with the band envelope between 2211 and 2195 cm^{-1} being replaced by a single broad band at 2152 cm^{-1}. Interestingly, the composed ν(C≡C) band pattern of **3d** itself is gradually converting along with the overall anodic decay to a single band at 2201 cm^{-1}. It seems clear that reduction of **3d** to [**3d**]$^{2-}$ results in a distribution of the extra electron density into orbitals that have significant nitrophenyl and alkynyl character.

In contrast to the nitrophenylene reduction, the reversible ferrocenyl-based oxidation of **3d** does not affect ν(C=C)$_{vinyl}$ or ν(C≡C) wavenumbers significantly, resulting in blue shifts smaller than 5 cm^{-1}, but with a substantial loss of intensity of these bands (Figure 7). These observations indicate that the Fc

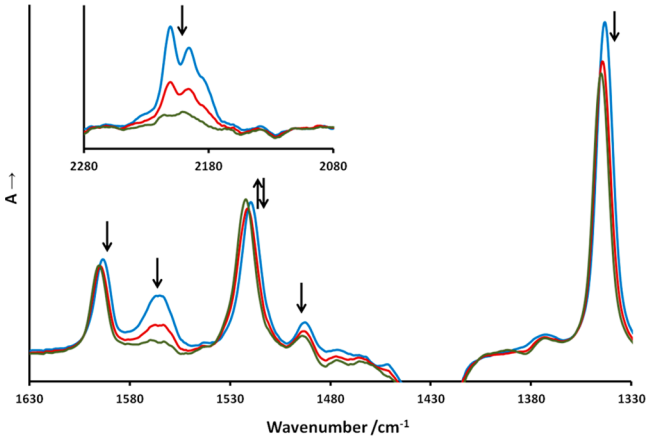

Figure 7. Reversible IR spectral changes resulting from the ferrocenyl-centered electrochemical oxidation of **3d** in $CH_2Cl_2/10^{-1}$ M Bu_4NPF_6 within an OTTLE cell. The inset documents the ν(C≡C) region. The spectral changes between 1410 and 1490 cm^{-1} are caused by fluctuations of the electrolyte absorption.

center has only a small influence on the structure of the cross-conjugated fragment and therefore does not interact strongly with the 1,1-dialkynylvinyl moiety.

Similar small IR spectral changes in the ν(C═C)$_{aryl}$ bands of the substituted phenyl groups, viz. tolyl (**3a**), *N*-methylanilinyl (**3b**), and *N*,*N*-dimethylanilinyl (**3c**), are observed in the course of oxidation of the ferrocenyl group in **3a**–**c**. However, the ν(C≡C) and ν(C═C)$_{vinyl}$ bands of **3a**–**c** with the donor substituents on the phenyl ring exhibit markedly different response to the 1e oxidation in comparison with **3d**. For the most stable derivative [**3a**]$^+$, the wavenumbers of the ν(C≡C) band maxima remain almost unchanged, while the ν(C═C)$_{vinyl}$ band at 1575 cm^{-1} shifts to lower energy by 16 cm^{-1} and the intensities of ν(C≡C) and ν(C═C)$_{vinyl}$ absorption bands both strongly increase in the cationic products (Figure S3, Supporting Information). Again, these qualitative changes in band intensity are consistent with a simple valence bond model for the changes in dipole moment across the molecule in response to localized changes in redox state.

For **3c**, the ferrocenyl-centered oxidation resulted in the gradual shift of the ν(C≡C) band envelope at 2185 cm^{-1} to a new structured band at 2173 cm^{-1} (Figure 8). However, in addition to the formation of [**3c**]$^+$, a new broad ν(C≡C) absorption at 2120 cm^{-1} was also observed to be independently growing, especially at later stages of the oxidation processes with concomitant decrease in the ν(C≡C) absorption of [**3c**]$^+$. This behavior reflects the reactivity of the aniline substituent in

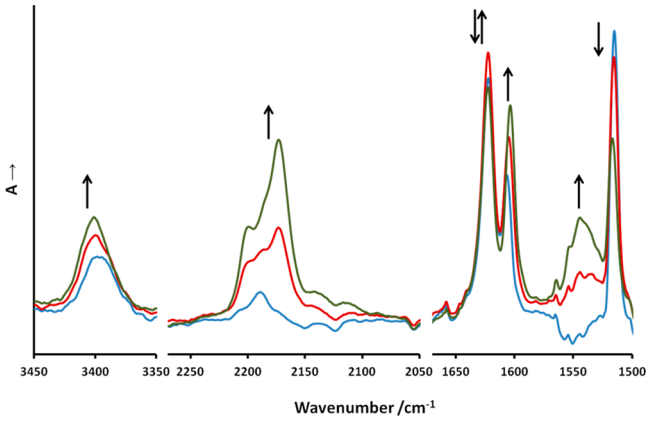

Figure 8. IR spectral changes resulting from the ferrocenyl-centered electrochemical oxidation of **3c** in $CH_2Cl_2/10^{-1}$ M Bu_4NPF_6 within an OTTLE cell, prior to the thermal decomposition of [**3c**]$^+$. The inset corresponds to the ν(N–H) region.

the cationic product, which may form an insoluble polyaniline-type structure. In contrast to the case for the parent **3c**, the ν(C═C)$_{vinyl}$ band of [**3c**]$^+$ is IR active in solution (1545 cm^{-1}) and is found some 14 cm^{-1} lower than in [**3a**]$^+$ (Table 1).

Finally, for the dimethylamino derivative **3b**, the IR spectral changes due to the ferrocenyl-centered oxidation show a trend very similar to that observed for **3c** (Figure S4 (Supporting Information), Table 1). The secondary reactivity of [**3b**]$^+$ is markedly less pronounced than noted above for [**3c**]$^+$, which can be ascribed to higher steric demands of the *N*,*N*-dimethylaniline substituents inhibiting the polymerization reaction in the cationic product. Ultimately, this process complicates the spectroelectrochemical study of **3b**,**c** due to severe passivation of the electrode surface. Nevertheless, as also seen in the solid-state ATR-FTIR spectra of the neutral systems, the ν(C═C)$_{vinyl}$ wavenumbers in the oxidized forms exhibit some substituent effects and are more sensitive to the ferrocenyl oxidation than the ν(C≡C) and ν(C═C)$_{aryl}$ modes, especially in the presence of a donor group on the phenyl rings.

UV–vis–near-IR spectral changes recorded for compounds **3a**–**d** in the course of their ferrocenyl-centered oxidation are shown in Figures 9 and 10 and Figures S5 and S6 (Supporting Information), and the wavenumbers of the absorption maxima of the neutral parent and oxidized cationic complexes are

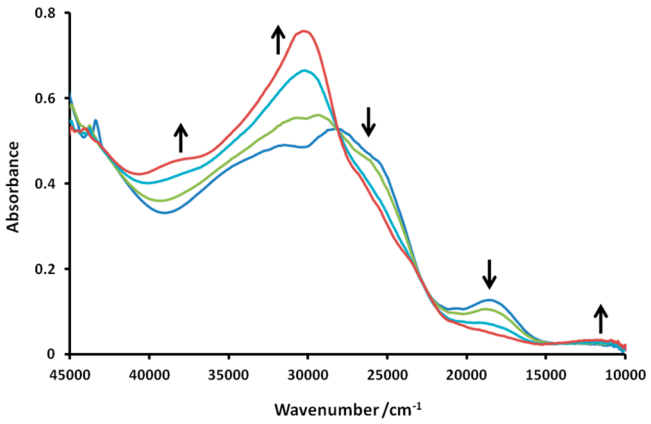

Figure 9. Reversible UV–vis–near-IR spectral changes resulting from the ferrocenyl-centered electrochemical oxidation of **3d** in $CH_2Cl_2/10^{-1}$ M Bu_4NPF_6 within an OTTLE cell.

dx.doi.org/10.1021/om400535y | *Organometallics* 2013, 32, 6022–6032

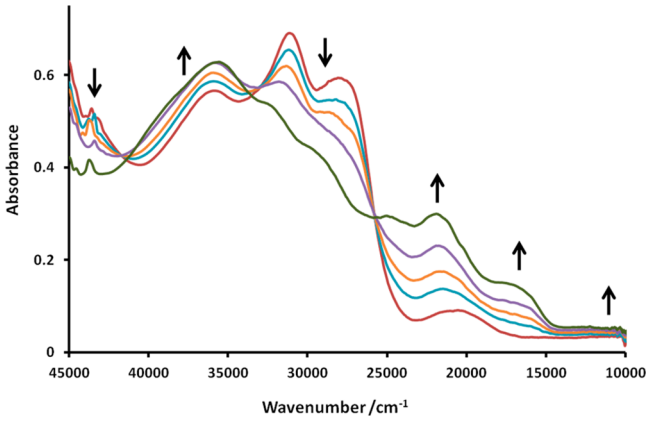

Figure 10. Reversible UV−vis−near-IR spectral changes resulting from the ferrocenyl-centered electrochemical oxidation of **3c** in $CH_2Cl_2/10^{-1}$ M Bu_4NPF_6 within an OTTLE cell.

summarized in Table 3. More detailed analyses of the spectral changes and assignments of the absorption bands to particular

Table 3. Electronic Absorption Spectra of 3a−d and Their 1e Oxidized Forms in CH_2Cl_2/Bu_4NPF_6

compd	wavenumber (cm^{-1})
3a	43420, 40020, 35210, 33170, 29730, 28900, 20160
3a$^+$	39250, 34730 (sh), 32440 (sh), 30340, 23300, 17730, ~10970
3b	43240, 34850, 30250 (sh), 27900 (sh), 26750, 20160
3b$^+$	39250, 34390, 30790 (sh), 27460, 19900, 15610, ~10480
3c	43610, 35830, 31070, 27750, 20790
3c$^+$	38660 (sh), 35820, 32340, 29070, 25080, 22000, 16470, ~10500
3d	35090, 31840, 28510, 25640, 18590
3d$^+$	38370, 30250, 26020 (sh), 23300 (sh), 18750, ~11040

vertical electronic transitions are facilitated by DFT and TDDFT calculations of the closed- and open-shell systems described below. The secondary reactivity of the oxidized anilinyl-substituted compounds $[\mathbf{3b}]^+$ and $[\mathbf{3c}]^+$ observed in the IR spectroelectrochemical experiments is prohibited at the much lower concentrations used for the anodic UV−vis spectroelectrochemical experiments (see the Experimental Section).

Computational Studies. To gain further insight into the electronic structure and the character of the electronic transitions, calculations at the density functional theory (DFT) level were performed using compounds $[\mathbf{3a}']^n$, $[\mathbf{3b}']^n$, and $[\mathbf{3d}']^n$ (n = 0, 1+) as representative examples (the $'$ notation is employed to distinguish the in silico system from the experimental complex). The BLYP35 functional (35% exact exchange admixture) was used together with the COSMO continuum solvent model (CH_2Cl_2; ε = 8.93).[27] This combination of methods is known to provide a reasonable description of electronic localization/delocalization and excited-state properties of open-shell organic and transition-metal systems, including the charge transfer characteristics of mixed-valence examples.[28]

The DFT calculations confirmed an essentially ferrocenyl-centered oxidation in each case for $[\mathbf{3a}']^+$, $[\mathbf{3b}']^+$, and $[\mathbf{3d}']^+$, with spin density almost exclusively localized on the ferrocenyl moiety (Tables S1−S7, Supporting Information). In the case of $[\mathbf{3b}']^+$ the calculated spin density on the ferrocenyl moiety (101%) is matched with a small negative contribution from the two ethynyl units (−1%) (Figure 11). Appreciable spin polarization is found at the chosen computational level, with appreciably negative (=β) spin density on the π orbitals of the cyclopentadienyl rings (−0.27 and −0.20, respectively) and mainly positive (=α) spin density on the iron atom (1.48). This spin polarization is accompanied by spin contamination ($\langle S^2\rangle$ = 0.88 compared to the nominal 0.75 for a doublet). This valence-shell spin polarization and spin contamination at the hybrid DFT level is consistent with a significant Fe−Cp antibonding character of the SOMO, as has been analyzed in detail for other 3d transition-metal complexes in the context of computing hyperfine couplings.[29]

The analysis of the spin-density distributions in terms of MOs is complicated by the strong spin polarization, which leads to violation of the Aufbau principle. For example the "true" singly occupied MO in $[\mathbf{3a}']^+$ is not the α (i.e., spin-up) spin orbital with the highest energy (which would be α-MO 115α) but rather is found at lower energy in the list of α-MOs (96α). An assignment of the proper "doubly occupied" MOs, and thus of the proper SOMO, was only possible after an overlap matching of the corresponding α- and β-MOs. The same holds for the other complexes. In view of these aspects, we will refrain from a detailed MO-based analysis but rather simply note that the α-SOMO of $[\mathbf{3a}']^+$ is ferrocenyl-based (90%), thus matching the spin density distribution qualitatively. The localization of the α-SOMO (and thus of the spin density) on Fc^+ is diminished in the presence of the donor substituents NMe_2 in $[\mathbf{3b}']^+$ (113α, 78%) (Figure 11) but somewhat enhanced by the electron-withdrawing NO_2 groups in $[\mathbf{3d}']^+$ (108α, 92%). We note also in passing that the SOMO involves σ-type orbitals on the cyclopentadienyl rings (Figure 11, right), in contrast with the π-type negative spin density arising from spin polarization (Figure 11, left).

Harmonic vibrational frequency calculations were performed on each member of the series $[\mathbf{3a}']^n$, $[\mathbf{3b}']^n$, and $[\mathbf{3d}']^n$ (n = 0, 1) (Table 1). In agreement with experimental spectroelectrochemical results, the ν(C≡C) frequencies of the neutral and the oxidized form differ little. For each oxidation state, two ν(C≡C) bands are computed. Taking $[\mathbf{3b}']^{n+}$ as an example, while the ν(C≡C) bands appear at 2223 and 2210 cm^{-1} for

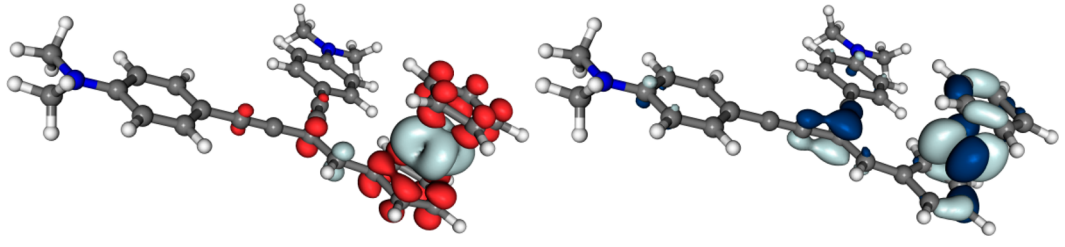

Figure 11. Isosurface plots of the spin density (±0.002 au, left) and the SOMO 113α (±0.03 au, right) of $[\mathbf{3b}']^+$.

dx.doi.org/10.1021/om400535y | *Organometallics* 2013, 32, 6022−6032

the neutral species **3b′**, upon oxidation to $[\mathbf{3b}']^+$ a small red shift to 2203 and 2178 cm^{-1} occurs. While the $\nu(C{\equiv}C)$ frequencies of 2210 cm^{-1} (**3b′**) and 2203 cm^{-1} ($[\mathbf{3b}']^+$) are in good agreement with the principal features of the experimental band envelopes (**3b**, 2188 cm^{-1}; $[\mathbf{3b}']^+$, 2167 cm^{-1}), the additional features at 2223 cm^{-1} (**3b′**) and 2203 cm^{-1} ($[\mathbf{3b}']^+$) may explain in part the experimentally observed high-energy shoulder of the $\nu(C{\equiv}C)$ band. Overall, the calculations in each case overestimate the $\nu(C{\equiv}C)$ frequencies slightly (in spite of the customary scaling by an empirical factor of 0.95, cf. Computational Details).

The calculated $\nu(C{=}C)_{aryl}$ frequencies are in excellent agreement with the experimental data across the series. Again, taking **3b′** by way of example, for neutral **3b′**, the DFT calculations give two nearly degenerate frequencies that correspond to the experimental features at 1607 cm^{-1} (**3b′**, 1613 and 1614 cm^{-1}), and 1522 cm^{-1} (**3b′**, 1514 and 1511 cm^{-1}). The same holds true for the cation $[\mathbf{3b}']^+$, with very small shifts in the calculated $\nu(C{=}C)_{aryl}$ frequencies on oxidation ($[\mathbf{3b}']^+$, 1611, 1604, 1518, and 1510 cm^{-1}). The main difference in the computed IR spectra of the neutral and oxidized forms is the appearance of an IR-active $\nu(C{=}C)_{vinyl}$ frequency at 1527 cm^{-1} for $[\mathbf{3b}']^+$, which corresponds to the experimental band at 1545 cm^{-1}. Overall, the very good agreement between the calculated and experimental vibrational features permits a degree of confidence in the optimized conformations and hence significance of the calculated electronic structures.

To assign the electronic transitions in the spectroelectrochemically observed UV−vis spectra, time-dependent DFT (TDDFT) calculations were performed for $[\mathbf{3a}']^+$, $[\mathbf{3b}']^+$, and $[\mathbf{3d}']^+$ (Table S8, Supporting Information). In each case the lowest energy excitation of significant intensity is computed to be between 8200 and 8400 cm^{-1}. It arises from a low-lying ferrocenyl-based MO and therefore has interconfigurational (or pseudo-dd) character. The first electronic transition above 10000 cm^{-1} is computed at 10123 cm^{-1} (μ_{trans} = 2.0 D) for $[\mathbf{3b}']^+$, which is in excellent agreement with the broad observed absorption at 10480 cm^{-1} for this complex and similar bands in the other species. Several orbitals contribute to the transition. The predominant character is that of a charge transfer from one ene-yne unit to the ferrocenyl cation, although the orbitals are more delocalized in the case of $[\mathbf{3d}']^+$ than in the other systems.

Multiple transitions close in energy are computed around 16500 cm^{-1}. They can be assigned to the broad feature observed experimentally near 15000 cm^{-1}. In the case of $[\mathbf{3b}']^+$ the excitations at 16108 cm^{-1} (μ_{trans} = 2.9 D) and at 16560 cm^{-1} (μ_{trans} = 6.2 D) arise from transitions in which the hole is transferred from the vinylferrocenyl moiety to one branch of the cross-conjugated organic fragment. At 16309 cm^{-1} (μ_{trans} = 3.4 D) TDDFT gives a purely ferrocenyl-centered excitation, which does not involve charge transfer. Precise assignment of the character of the excitation at 16678 cm^{-1} (μ_{trans} = 3.8 D) is not straightforward, as multiple transitions of both charge-transfer (CT) and interconfigurational character contribute to the absorption feature (Table S8, Supporting Information).

The most intense excitation in $[\mathbf{3b}']^+$ (μ_{trans} = 7.2 D), computed at 19640 cm^{-1}, has again ene-yne to metal charge-transfer character. The excitation energy of 19640 cm^{-1} corresponds well with the band at 19900 cm^{-1} determined experimentally. This band exhibits a weak shoulder, which can be attributed to a computed low-intensity transition at 20127 cm^{-1} (μ_{trans} = 1.5 D). Similar conclusions can also be drawn from the TDDFT results for $[\mathbf{3a}']^+$ and $[\mathbf{3d}']^+$.

CONCLUSION

A simple preparative route to ferrocenyl-substituted 1,1-bis(alkynyl)ethenes has been developed. The alkynyl substituents have a modest electronic influence on the ferrocenyl moiety, to which they are linearly coupled, as is evidenced by the sensitivity of the ferrocenyl oxidation potential to the electronic character of these remote groups. The modest shift in $\nu(C{\equiv}C)$ and $\nu(C{=}C)_{vinyl}$ bands in response to the oxidation state of the ferrocene moiety together with the presence of a number of charge transfer transitions in the spectra of $[\mathbf{3a}]^+$, $[\mathbf{3b}]^+$, and $[\mathbf{3d}]^+$ also points to a small interaction between the metallocene and cross-conjugated fragments. However, strong ground state electronic coupling is not an essential criterion from the point of view of the Grozema molecular transistor designs, and the limited structural rearrangement (evidenced by the small $\nu(CC)$ variations in response to charge state changes) may also help both preserving QI effects and aiding integration into molecular electronic circuits, where large structural changes during operation would be detrimental to long-term device stability.

EXPERIMENTAL SECTION

All reactions were carried out under an atmosphere of nitrogen using standard Schlenk techniques as a matter of routine, although no special precautions were taken to exclude air or moisture during workup. Solvents were purified and dried using an Innovative Technology SPS-400 instrument and degassed before use. The compounds $Pd(PPh_3)_4$[30] and ethynylferrocene[19b] were prepared by the literature methods. CBr_4 was purified by sublimation before use. Other reagents were purchased and used as received.

NMR spectra were recorded on a Bruker Avance (^1H, 400.13 MHz; $^{13}C\{^1H\}$, 100.61 MHz) spectrometer from $CDCl_3$ solutions unless otherwise indicated and referenced against solvent resonances ($CDCl_3$, ^1H 7.26 ^{13}C 77.0; CH_2Cl_2, ^{13}C 54.00). NMR labeling schemes are given in Figure 2 and the Supporting Information. IR spectra were recorded using a Nicolet 6700 spectrometer from cells fitted with CaF_2 windows (CH_2Cl_2) and a Perkin-Elmer Spectro 100 FTIR spectrometer equipped with a universal ATR sampling accessory (solid state), respectively. ASAP mass spectra were recorded from solid aliquots on an LCT Premier XE mass spectrometer (Waters Ltd., U.K.) or Xevo QToF mass spectrometer (Waters Ltd., U.K.) in which the aliquot is vaporized using hot N_2, ionized by a corona discharge, and carried to the TOF detector (working range m/z 100−1000).

The supporting electrolyte, tetrabutylammonium hexafluorophosphate (Bu_4NPF_6, Aldrich), was recrystallized twice from absolute ethanol and dried overnight under vacuum at 80 °C before use. IR and UV−vis spectra were recorded on a Bruker Vertex 70v FT-IR spectrometer and a Scinco S3100 diode array spectrophotometer, respectively. UV−vis−near-IR−IR spectroelectrochemical experiments at room temperature were conducted with an OTTLE cell equipped with a Pt-minigrid working electrode and CaF_2 windows.[31] The optical path of the cell was ca. 0.2 mm. Controlled-potential electrolyses within the OTTLE cell were carried out using a PA4 potentiostat (Laboratory Devices, Polná, Czech Republic). The concentrations of the ferrocenyl compounds and the supporting electrolyte used in these measurements were 1.3 × 10^{-2} and 3 × 10^{-1} mol dm^{-3} for IR spectroelectrochemical experiments and 10^{-3} and 3 × 10^{-1} mol dm^{-3} for the UV−vis−near-IR studies, respectively.

Preparation of 2.[19b] CBr_4 (1.936 g, 5.84 mmol) and PPh_3 (3.062 g, 11.68 mmol) in degassed dry CH_2Cl_2 (50 mL) were stirred at 0 °C for 15 min until the solution was deep orange. At this point FcCHO (1.00 g, 4.67 mmol) was added to the solution. The solution was stirred for 30 min, the ice bath was removed, and stirring was continued for a further 2 h. The mixture was then treated with hexane

dx.doi.org/10.1021/om400535y | Organometallics 2013, 32, 6022−6032

to precipitate the phosphine products and filtered. The solid was redissolved and precipitated again with hexane and the process repeated until the washings ran clear. The hexane solutions were combined, and the solvent was removed in vacuo. The crude material was purified by silica column chromatography with hexane as eluent, and the solvent was removed from the bright red band to give a red oil that solidified on standing. Yield: 1.4 g, 82%. Spectroscopic data were identical with those reported previously.[19b]

Preparation of 3a−e. *General Procedure.* In an oven-dried flask triethylamine (15 mL) was added and the solvent degassed. To the solution were added CuI (5 mg), $Pd(PPh_3)_4$ (32 mg, 0.027 mmol), **2** (200 mg, 0.054 mmol), and **4**, and the mixture was refluxed for 17 h. The mixture was filtered and the solvent removed under reduced pressure. The crude mixture was purified with silica column chromatography with hexane increasing to hexane/CH_2Cl_2 (70/30) as eluent; removal of the solvent gave the desired compound.

*Compound **3a**.* From **4a** (157 mg, 1.35 mmol), obtained as a dark red solid. Yield: 109 mg, 46%. ^{1}H NMR (CD_2Cl_2): δ 2.36 (3H, s, Me); 2.39 (3H, s, Me); 4.21 (5H, s, Cp); 4.41 (2H, apparent t, J = 2 Hz, C_5H_4); 4.90 (2H, apparent t, J = 2 Hz); 6.95 (1H, s, C*H*═); 7.14 (2H, d, J = 8 Hz, C_6H_4); 7.20 (2H, d, J = 8 Hz, C_6H_4); 7.41 (2H, d, J = 8 Hz, C_6H_4); 7.49 (2H, d, J = 8 Hz, C_6H_4). ^{13}C NMR (CD_2Cl_2): δ 21.80 (C_m); 21.85 (C_t); 70.20 (C_a); 70.37 (C_c); 71.10 (C_b); 80.28 (C_d); 87.75 (C_p); 87.84 ($C_{g/n}$); 89.46 (C_f); 94.09 (C_i); 99.76 ($C_{g/n}$); 120.74 (C_o); 120.76 (C_h); 129.74 (C_r); 129.87 (C_k); 131.72 (C_q); 131.75 (C_j); 139.09 (C_s); 139.50 (C_l); 144.82 (C_e). Anal. Found: C, 81.87; H 5.41. Calcd: C, 81.81; H, 5.50. ASAP-MS(+): m/z 440.1 $[M]^+$.

*Compound **3b**.* From **4b** (17 mg, 1.36 mmol), obtained as a red solid. Yield: 109 mg, 40%. ^{1}H NMR (CD_2Cl_2): δ 2.98 (6H, s, NMe_2); 3.01 (6H, s, NMe_2); 4.20 (5H, s, Cp); 4.35 (2H, apparent t, J = 2 Hz, C_5H_4); 4.89 (2H, apparent t, J = 2 Hz, C_5H_4); 6.64 (2H, d, J = 9 Hz, C_6H_4); 6.70 (2H, d, J = 9 Hz, C_6H_4); 6.83 (1H, s, C*H*═); 7.39 (2H, d, J = 9 Hz, C_6H_4); 7.47 (2H, d, J = 9 Hz, C_6H_4). ^{13}C NMR (CD_2Cl_2): δ 40.38 (C_m, C_t); 69.93 (C_a); 70.45 (C_c); 80.87 (C_b); 86.59 ($C_{g/n}$); 88.18 (C_f); 88.51 (C_p); 95.01 (C_i); 100.89 ($C_{g/n}$); 110.24 (C_h); 110.25 (C_o); 112.20 (C_r); 112.26 (C_k); 132.75 (C_j); 132.78 (C_q); 141.64 (C_e); 150.56 (C_s); 150.77 (C_l). Anal. Found: C, 77.04; H, 6.13; N, 5.64. Calcd: C, 77.09; H, 6.07; N, 5.62. ASAP-MS(+): m/z 498.1 $[M]^+$.

*Compound **3c**.* From **4c** (250 mg, 2.13 mmol), obtained as a bright red solid. Yield: 236 mg, 55%. ^{1}H NMR (CD_2Cl_2): δ 3.83 (4H, s, 2 × NH_2); 4.20 (5H, s, Cp); 4.37 (2H, apparent t, J = 2 Hz, C_5H_4); 4.89 (2H, apparent t, J = 8 Hz); 6.62 (2H, d, J = 8 Hz, C_6H_4); 6.66 (2H, d, J = 8 Hz, C_6H_4); 6.85 (1H, s, C*H*═); 7.32 (2H, d, J = 8 Hz, C_6H_4); 7.39 (2H, d, J = 8 Hz, C_6H_4). ^{13}C NMR (CD_2Cl_2): δ 70.10 (C_a); 70.12 (C_c); 70.73 (C_b); 80.77 (C_d); 86.53 (C_f); 88.18 ($C_{g/n}$); 88.30 (C_h); 94.72 (C_o); 100.63 ($C_{g/n}$); 112.77 ($C_{l/s}$); 112.78 ($C_{l/s}$); 115.13 (C_k); 115.18 (C_r); 133.17 (C_q); 133.20 (C_j); 142.60 (C_e); 147.59 (C_i); 147.89 (C_p). Anal. Found: C, 75.87; H, 4.91; N, 6.44. Calcd: C, 76.19; H, 4.91; N, 6.44. ASAP-MS(+): m/z 443.1 $[M + H]^+$.

*Compound **3d**.* From **4d** (200 mg, 1.35 mmol), obtained as a dark red solid. Yield: 121 mg, 45%. Crystals suitable for X-ray diffraction were grown from CH_2Cl_2/ethanol. ^{1}H NMR (CD_2Cl_2): δ 4.25 (5H, s, Cp); 4.55 (2H, apparent t, J = 2 Hz, C_5H_4), 4.90 (2H, apparent t, J = 2 Hz, C_5H_4); 7.18 (1H, s, C*H*═), 7.65 (2H, d, J = 9 Hz, C_6H_4); 7.72 (2H, d, J = 9 Hz, C_6H_4); 8.22 (2H, d, J = 9 Hz, C_6H_4); 8.27 (2H, d, J = 9 Hz, C_6H_4). ^{13}C NMR (CD_2Cl_2): δ 69.92 (C_a); 70.28 (C_c); 71.67 (C_b); 78.66 (C_d); 86.03 (C_p); 91.70 (C_i); 92.29 ($C_{g/n}$); 94.24 (C_f); 96.85 ($C_{g/n}$); 123.63 (C_r); 123.76 (C_k); 129.85 (C_h); 130.07 (C_o); 131.91 (C_q); 131.94 (C_j), 146.83 (C_s), 147.10 (C_l), 149.12 (C_e). ASAP-MS(+): m/z 502.1.

*Compound **Z-5d**.* Silica column chromatography of the previous reaction with hexane increasing to hexane/CH_2Cl_2 (70/30) as eluent and removal of the solvent gave the title compound as a dark red solid. Yield: 49 mg. Due to the facile E/Z isomerization of the system ^{13}C NMR could not be obtained. Crystals suitable for X-ray diffraction were grown from CH_2Cl_2/ethanol. ^{1}H NMR ($CDCl_3$): δ 4.23 (5H, s, Cp); 4.45 (2H, apparent t, J = 2 Hz, C_5H_4), 4.85 (2H, apparent t, J = 2 Hz, C_5H_4), 7.19 (1H, s, C*H*═), 7.62 (2H, d, J = 9 Hz, C_6H_4), 8.22 (2H, d, J = 9 Hz, C_6H_4).

*Compound **3e**.* From **4e** (0.42 mL, 2.98 mmol), obtained as a dark red oil. Yield: 416 mg, 76%. ^{1}H NMR (CD_2Cl_2): δ 0.22 (9H, s, $SiMe_3$); 0.29 (9H, s, $SiMe_3$); 4.19 (5H, s, Cp); 4.38 (2H, apparent t, J = 2 Hz), 4.83 (2H, apparent t, J = 2 Hz); 6.89 (1H, s, C*H* dbd=). ^{13}C NMR (CD_2Cl_2): δ 0.06 (C_l), 0.11 (C_i), 70.18 (C_a), 70.50 (C_c), 71.14 (C_b), 79.58 (C_d), 92.57 (C_k), 99.30 (C_h), 100.16 ($C_{g/j}$), 103.21 ($C_{g/j}$), 105.00 (C_f), 147.78 (C_e). ASAP-MS(+): m/z 404.1 $[M]^+$.

Preparation of 3f. To a stirred solution of **3e** (0.345 g, 0.853 mmol) in MeOH (10 mL) and THF (10 mL) was added K_2CO_3 (0.589 g, 4.265 mmol), and the reaction mixture was stirred for 2 h. The mixture was poured into H_2O (20 mL) and extracted with CH_2Cl_2 (3 × 15 mL), and the organic phases were combined, dried over $MgSO_4$, and filtered. The solvent was removed in vacuo to give a bright red oil that solidified on standing. Yield: 209 mg, 94%. ^{1}H NMR (CD_2Cl_2): δ 3.05 (1H, s, ≡CH); 3.45 (1H, s, ≡CH); 4.19 (5H, s, Cp); 4.42 (2H, apparent t, J = 2 Hz), 4.84 (2H, apparent t, J = 2 Hz); 7.00 (1H, s, C*H*═). ^{13}C NMR (CD_2Cl_2): δ 70.21 (C_a); 70.52 (C_c); 71.30 (C_b); 75.77 (C_i); 79.05 (C_d); 81.87 ($C_{g/i}$); 82.76 (C_h), 83.69 ($C_{g/i}$); 96.91 (C_f); 148.49 (C_e). ASAP MS(+): m/z 261.0 $[M + H]^+$.

X-ray Crystallography. Single-crystal X-ray data were collected at 120 K on Bruker SMART CCD 6000 (**3d**) and Agilent Gemini S-Ultra (**Z-5d**) diffractometers equipped with Cryostream (Oxford Cryosystems) open-flow nitrogen cooling devices using graphite-monochromated Mo Kα radiation (λ = 0.71073 Å). Both structures were solved by direct methods and refined by full-matrix least squares on F^2 for all data using SHELXL[32] and OLEX2[33] software. All non-hydrogen atoms were refined with anisotropic displacement parameters; H atoms were found in the difference Fourier synthesis and refined isotropically. Crystallographic data for the structures have been deposited with the Cambridge Crystallographic Data Centre as supplementary publications CCDC-950424 and 950425.

Computational Details. All ground-state structures and properties and subsequent TDDFT were computed using a version of the TURBOMOLE 6.4 code[34] locally modified by the Berlin group. All DFT calculations reported in the paper were performed with the global hybrid functional BLYP35.[35]

$$E_{XC} = 0.65(E_X^{LSDA} + \Delta E_X^{B88}) + 0.35E_X^{exact} + E_C^{LYP}$$

While not a thermochemically optimized functional, BLYP35 has been shown to provide a good balance between reduced self-interaction errors and a simulation of static correlation, thus providing good agreement with ground- and excited-state experimental data for organic mixed-valence systems,[36] as well as for mixed-valence transition-metal complexes.[28c] As experiments were mainly carried out in dichloromethane (permittivity ε = 8.93), this solvent was considered by the conductor-like screening solvent model (COSMO) in TURBOMOLE 6.4.[37] For all calculations, split-valence basis sets def2-SVP were employed.[38] Calculated harmonic vibrational frequencies were scaled by an empirical factor of 0.95.[39] Spin density and molecular orbital plots were obtained using the Molekel program.[40]

■ ASSOCIATED CONTENT

Supporting Information

Figures, tables, and CIF files giving NMR labeling schemes for **3e,f**, ATR-FTIR spectra of **3a−d**, IR and UV−vis−near-IR spectra of **3a,b** during oxidation in a spectroelectrochemical cell, atomic coordinates and selected bond lengths and angles for all optimized geometries, orbital energies, and Mulliken population analyses of $[\mathbf{3a}']^+$, $[\mathbf{3b}']^+$, and $[\mathbf{3d}']^+$, calculated transition energies E_{trans}, transition dipole moments μ_{trans}, and character of $[\mathbf{3a}']^+$, $[\mathbf{3b}']^+$, and $[\mathbf{3d}']^+$, crystallographic refinement details, and crystallographic data for **3d** and **Z-5d**. This material is available free of charge via the Internet at http://pubs.acs.org.

AUTHOR INFORMATION

Corresponding Author

*E-mail: paul.low@uwa.edu.au (P.J.L.); martin.kaupp@tu-berlin.de (M.K.); f.hartl@reading.ac.uk (F.H.).

Author Contributions

The manuscript was written through contributions of all authors. All authors have given approval to the final version of the manuscript.

Notes

The authors declare no competing financial interest.

ACKNOWLEDGMENTS

M.P. gratefully acknowledges the German Academic Exchange Service (DAAD) for a travel scholarship. P.J.L. held an EPSRC Leadership Fellowship and currently holds an ARC Future Fellowship (FT120100073). This work was supported by the ARC (FT120100073), the EPSRC (EP/K00753X/1; EP/H005595/1), the Berlin DFG cluster of excellence on "Unifying Concepts in Catalysis" (UniCat), and the DFG (KA1187/13-1).

REFERENCES

(1) (a) Creutz, C. *Prog. Inorg. Chem.* **1983**, *30*, 1. (b) Crutchley, R. J. *Adv. Inorg. Chem.* **1994**, *41*, 273. (c) Low, P. J.; Brown, N. J. *J. Cluster Sci.* **2010**, *21*, 235. (d) Launay, J.-P. *Coord. Chem. Rev.* **2013**, *257*, 1544. (e) Halet, J. F.; Lapinte, C. *Coord. Chem. Rev.* **2013**, *257*, 1584. (f) Heckmann, A.; Lambert, C. *Angew. Chem., Int. Ed.* **2012**, *51*, 326. (g) Hankache, J.; Wenger, O. S. *Chem. Rev.* **2011**, *111*, 5138. (h) Glover, S. D.; Goeltz, J. C.; Lear, B. J.; Kubiak, C. P. *Coord. Chem. Rev.* **2010**, *254*, 331. (i) Kubiak, C. P. *Inorg. Chem.* **2013**, *52*, 5663.

(2) (a) Brady, M.; Weng, W.; Gladysz, J. A. *J. Chem. Soc., Chem. Commun.* **1994**, 2655. (b) Mohr, W.; Stahl, J.; Hampel, F.; Gladysz, J. A. *Inorg. Chem.* **2001**, *40*, 3263. (c) Mohr, W.; Stahl, J.; Hampel, F.; Gladysz, J. A. *Chem. Eur. J.* **2003**, *9*, 3324. (d) Owen, G. R.; Stahl, J.; Hampel, F.; Gladysz, J. A. *Organometallics* **2004**, *23*, 5889. (e) Zheng, Q.; Hampel, F.; Gladysz, J. A. *Organometallics* **2004**, *23*, 5896. (f) Owen, G. R.; Hampel, F.; Gladysz, J. A. *Organometallics* **2004**, *23*, 5893. (g) de Quadras, L.; Hampel, F.; Gladysz, J. A. *Dalton Trans.* **2006**, 2929. (h) Zheng, Q.; Bohling, J. C.; Peters, T. B.; Frisch, A. C.; Hampel, F.; Gladysz, J. A. *Chem. Eur. J.* **2006**, *12*, 6486. (i) de Quadras, L.; Bauer, E. B.; Stahl, J.; Zhuravlev, F.; Hampel, F.; Gladysz, J. A. *New J. Chem.* **2007**, *31*, 1594. (j) de Quadras, L.; Bauer, E. B.; Mohr, W.; Bohling, J. C.; Peters, T. B.; Martín-Alvarez, J. M.; Hampel, F.; Gladysz, J. A. *J. Am. Chem. Soc.* **2007**, *129*, 8296. (k) Stahl, J.; Mohr, W.; de Quadras, L.; Peters, T. B.; Bohling, J. C.; Martín-Alvarez, J. M.; Owen, G. R.; Hampel, F.; Gladysz, J. A. *J. Am. Chem. Soc.* **2007**, *129*, 8282. (l) Stahl, J.; Bohling, J. C.; Peters, T. B.; de Quadras, L.; Gladysz, J. A. *Pure Appl. Chem.* **2008**, *80*, 459. (m) Antonova, A. B.; Bruce, M. I.; Ellis, B. G.; Gaudio, M.; Humphrey, P. A.; Jevric, M.; Melino, G.; Nicholson, B. K.; Perkins, G. J.; Skelton, B. W.; Stapleton, B.; White, A. H.; Zaitseva, N. N. *Chem. Commun.* **2004**, 960. (n) Coat, F.; Lapinte, C. *Organometallics* **1996**, *15*, 477. (o) Xi, B.; Xu, G. L.; Fanwick, P. E.; Ren, T. *Organometallics* **2009**, *28*, 2338. (p) Xu, G. L.; Xi, B.; Updegraff, J. B.; Protasiewicz, J. D.; Ren, T. *Organometallics* **2006**, *25*, 5213.

(3) (a) Lissel, F.; Fox, T.; Blacque, O.; Polit, W.; Winter, R. F.; Vekatesan, K.; Berke, H. *J. Am. Chem. Soc.* **2013**, *135*, 4051. (b) Semenov, S. N.; Taghipourian, S. F.; Blacque, O.; Fox, T.; Venkatesan, K.; Berke, H. *J. Am. Chem. Soc.* **2010**, *132*, 7584. (c) Semenov, S. N.; Blacque, O.; Fox, T.; Venkatesan, K.; Berke, H. *J. Am. Chem. Soc.* **2010**, *132*, 3115.

(4) (a) Low, P. J.; Rousseau, R.; Lam, P.; Udachin, K. A.; Enright, G. D.; Tse, J. S.; Wayner, D. D. M.; Carty, A. J. *Organometallics* **1999**, *18*, 3885. (b) Bruce, M. I.; Low, P. J.; Costuas, K.; Halet, J.-F.; Best, S. P.; Heath, G. A. *J. Am. Chem. Soc.* **2000**, *122*, 1949. (c) Bruce, M. I.; Ellis, B. G.; Low, P. J.; Skelton, B. W.; White, A. H. *Organometallics* **2003**, *22*, 3184. (d) Bruce, M. I.; Costuas, K.; Davin, T.; Ellis, B. G.; Halet, J.-F.; Lapinte, C.; Low, P. J.; Smith, M. E.; Skelton, B. W.; Toupet, L.; White, A. H. *Organometallics* **2005**, *24*, 3864. (e) Bruce, M. I.; Costuas, K.; Ellis, B. G.; Halet, J.-F.; Low, P. J.; Moubaraki, B.; Murray, K. S.; Ouddai, N.; Perkins, G. J.; Skelton, B. W.; White, A. H. *Organometallics* **2007**, *26*, 3735. (f) Bruce, M. I.; Costuas, K.; Davin, T.; Halet, J.-F.; Kramarczuk, K. A.; Low, P. J.; Nicholson, B. K.; Perkins, G. J.; Roberts, R. L.; Skelton, B. W.; Smith, M. E.; White, A. H. *Dalton Trans.* **2007**, 5387. (g) Fitzgerald, E. C.; Brown, N. J.; Edge, R.; Helliwell, M.; Roberts, H. N.; Tuna, F.; Beeby, A.; Collison, D.; Low, P. J.; Whiteley, M. W. *Organometallics* **2012**, *31*, 157.

(5) (a) Le Narvor, N.; Toupet, L.; Lapinte, C. *J. Am. Chem. Soc.* **1995**, *117*, 7129. (b) Coat, F.; Lapinte, C. *Organometallics* **1996**, *15*, 477. (c) Coat, F.; Guillevic, M. A.; Toupet, L.; Paul, F.; Lapinte, C. *Organometallics* **1997**, *16*, 5988. (d) Guillemot, M.; Toupet, L.; Lapinte, C. *Organometallics* **1998**, *17*, 1928. (e) Paul, F.; Meyer, W. E.; Toupet, L.; Jiao, H. J.; Gladysz, J. A.; Lapinte, C. *J. Am. Chem. Soc.* **2000**, *122*, 9405. (f) Jiao, H. J.; Costuas, K.; Gladysz, J. A.; Halet, J.-F.; Guillemot, M.; Toupet, L.; Paul, F.; Lapinte, C. *J. Am. Chem. Soc.* **2003**, *125*, 9511. (g) Ibn Ghazala, S.; Paul, F.; Toupet, L.; Roisnel, T.; Hapiot, P.; Lapinte, C. *J. Am. Chem. Soc.* **2006**, *128*, 2463. (h) Szafert, S.; Paul, F.; Meyer, W. E.; Gladysz, J. A.; Lapinte, C. *C. R. Chem.* **2008**, *11*, 693.

(6) (a) Zhou, Y.; Seyler, J. W.; Weng, W.; Arif, A. M.; Gladysz, J. A. *J. Am. Chem. Soc.* **1993**, *115*, 8509. (b) Brady, M.; Weng, W.; Zhou, Y.; Seyler, J. W.; Amoroso, A. J.; Arif, A. M.; Böhme, M.; Frenking, G.; Gladysz, J. A. *J. Am. Chem. Soc.* **1997**, *119*, 775. (c) Zhuravlev, F.; Gladysz, J. A. *Chem. Eur. J.* **2004**, *10*, 6510. (d) Herrmann, C.; Neugebauer, J.; Gladysz, J. A.; Reiher, M. *Inorg. Chem.* **2005**, *44*, 6174.

(7) (a) Ren, T.; Zou, G.; Alvarez, J. C. *Chem. Commun.* **2000**, 1197. (b) Xu, G.-L.; Zou, G.; Ni, Y.-H.; DeRosa, M. C.; Crutchley, R. J.; Ren, T. *J. Am. Chem. Soc.* **2003**, *125*, 10057. (c) Xu, G. L.; Crutchley, R. J.; DeRosa, M. C.; Pan, Q. J.; Zhang, H. X.; Wang, X. P.; Ren, T. *J. Am. Chem. Soc.* **2005**, *127*, 13354. (d) Xi, B.; Ren, T. *C.R. Chem.* **2009**, *12*, 321. (e) Ying, J. W.; Liu, I. P. C.; Xi, B.; Song, Y.; Campana, C.; Zuo, J. L.; Ren, T. *Angew. Chem., Int. Ed.* **2010**, *49*, 954. (f) Xi, B.; Liu, I. P. C.; Xu, G. L.; Choudhuri, M. M. R.; DeRosa, M. C.; Crutchley, R. J.; Ren, T. *J. Am. Chem. Soc.* **2011**, *133*, 15094.

(8) Ricks, A. B.; Solomon, G. C.; Colvin, M. T.; Scott, A. M.; Chen, K.; Ratner, M. A.; Wasielewski, M. R. *J. Am. Chem. Soc.* **2010**, *132*, 7973.

(9) (a) Campbell, K.; McDonald, R.; Tykwinski, R. R. *J. Org. Chem.* **2002**, *67*, 1133. (b) Campbell, K.; McDonald, R.; Tykwinski, R. R. *J. Porphyrins Phthalocyanines* **2005**, *9*, 794. (c) Ooms, K. J.; Campbell, K.; Tykwinski, R. R.; Wasylishen, R. E. *J. Mater. Chem.* **2005**, *15*, 4318.

(10) (a) Boldi, A. M.; Diederich, F. *Angew. Chem., Int. Ed. Engl.* **1994**, *33*, 468. (b) Anthony, J.; Boldi, A. M.; Boudon, C.; Gisselbrecht, J.-P.; Gross, M.; Seiler, P.; Knobler, C. B.; Diederich, F. *Helv. Chim. Acta* **1995**, *78*, 797. (c) Eisler, S.; Tykwinski, R. R. *Angew. Chem., Int. Ed.* **1999**, *38*, 1940. (d) Tobe, Y.; Umeda, R.; Iwasa, N.; Sonoda, M. *Chem. Eur. J.* **2003**, *9*, 5549. (e) Zhao, Y.-L.; Liu, Q.; Zhang, J.-P.; Liu, Z.-Q. *J. Org. Chem.* **2005**, *70*, 6913. (f) Bandyopahyay, A.; Varghese, B.; Hopf, H.; Sankararaman, S. *Chem. Eur. J.* **2007**, *13*, 3813. (g) Chen, G.; Wang, L.; Thompson, D. W.; Zhao, Y. *Org. Lett.* **2008**, *10*, 657. (h) Gholami, M.; Chaur, M. N.; Wilde, M.; Ferguson, M. J.; McDonald, R.; Echegoyen, L.; Tykwinski, R. R. *Chem. Commun.* **2009**, 3038. (i) Chen, G.; Dawe, L.; Wang, L.; Zhao, Y. *Org. Lett.* **2009**, *11*, 2736. (j) Hasegawa, M.; Takatsuka, Y.; Kuwatani, Y.; Mazaki, Y. *Tetrahedron Lett.* **2012**, *53*, 5385. (k) Linkcke, K.; Frellsen, A. F.; Parker, C. R.; Bond, A. D.; Hammerich, O.; Nielsen, M. B. *Angew. Chem., Int. Ed.* **2012**, *51*, 6099.

(11) (a) Anthony, J.; Boldi, A. M.; Rubin, Y.; Hobi, M.; Gramlich, V.; Knobler, C. B.; Seiler, P.; Diederich, F. *Helv. Chim. Acta* **1995**, *78*, 13. (b) Tykwinski, R. R.; Schreiber, M.; Gramlich, V.; Seiler, P.; Diederich, F. *Adv. Mater.* **1996**, *8*, 226. (c) Tykwinski, R. R.; Schreiber, M.; Perez Carlon, R.; Diederich, F.; Gramlich, V. *Helv. Chim. Acta* **1996**, *79*, 2249. (d) Tykwinski, R. R.; Hilger, A.; Diederich, F.; Luthi, H. P.; Seiler, P.; Gramlich, V.; Gisselbrecht, J. P.; Boudon, C.; Gross, M. *Helv. Chim. Acta* **2000**, *83*, 1484. (e) Diederich, F. *Chem. Commun.* **2001**,

219. (f) Gobbi, L.; Seiler, P.; Diederich, F.; Gramlich, V.; Boudon, C.; Gisselbrecht, J.-P.; Gross, M. *Helv. Chim. Acta* **2001**, *84*, 743. (g) Lu, W.; Zhu, N.; Che, C.-M. *J. Organomet. Chem.* **2003**, *670*, 11. (h) Koentjoro, O. F.; Zuber, P.; Puschmann, H.; Goeta, A. E.; Howard, J. A. K.; Low, P. J. *J. Organomet. Chem.* **2003**, *670*, 178.

(12) (a) Burdett, J. K.; Mortara, A. K. *Chem. Mater.* **1997**, *9*, 812. (b) Gobbi, L.; Seiler, P.; Diederich, F.; Gramlich, V. *Helv. Chim. Acta* **2000**, *83*, 1711. (c) Gobbi, L.; Elmaci, N.; Nuran, H. P.; Diederich, F. *ChemPhysChem* **2001**, *2*, 423. (d) Zhao, Y.; Ciulei, S. C.; Tykwinski, R. R. *Tetrahedron Lett.* **2001**, *42*, 7721. (e) Moonen, N. N. P.; Boudon, C.; Gisselbrecht, J.-P.; Seiler, P.; Gross, M.; Diederich, F. *Angew. Chem., Int. Ed.* **2002**, *41*, 3044. (f) Moonen, N. N. P.; Gist, R.; Boudon, C.; Gisselbrecht, J. P.; Seiler, P.; Kawai, T.; Kishioka, A.; Gross, M.; Irie, M.; Diederich, F. *Org. Biomol. Chem.* **2003**, *1*, 2032. (g) Mitzel, F.; Boudon, C.; Gisselbrecht, J.-P.; Seiler, P.; Gross, M.; Diederich, F. *Helv. Chim. Acta* **2004**, *87*, 1130. (h) Auffrant, A.; Diederich, F.; Boudon, C.; Gisselbrecht, J.-P.; Gross, M. *Helv. Chim. Acta* **2004**, *87*, 3085. (i) Zhao, Y.; Slepkov, A. D.; Akoto, C. O.; McDonald, R.; Hegmann, F. A.; Tykwinski, R. R. *Chem. Eur. J.* **2005**, *11*, 321. (j) Zhao, Y.; Zhou, N.; Slepkov, A. D.; Ciulei, S. C.; McDonald, R.; Hegmann, F. A.; Tykwinski, R. R. *Helv. Chim. Acta* **2007**, *90*, 909. (k) Bures, F.; Schweizer, W. B.; May, J.; Boudon, C.; Gisselbrecht, J.-P.; Gross, M.; Biaggio, I.; Diederich, F. *Chem. Eur. J.* **2007**, *13*, 5378. (l) Andersson, A. S.; Kerndrup, L.; Madsen, A. O.; Kilsa, K.; Brondsted Nielsen, M.; La Porta, P. R.; Biaggio, I. *J. Org. Chem.* **2009**, *74*, 375. (m) Kato, S.-i.; Kivala, M.; Schweizer, W. B.; Boudon, C.; Gisselbrecht, J.-P.; Diederich, F. *Chem. Eur. J.* **2009**, *15*, 8687. (n) Lincke, K.; Christensen, M. A.; Diederich, F.; Nielsen, M. B. *Helv. Chim. Acta* **2011**, *94*, 1743. (o) Hasegawa, M.; Takatsuka, Y.; Kuwatani, Y.; Mazaki, Y. *Tetrahedron Lett.* **2012**, *53*, 5385. (p) Bouit, P.-A.; Marszalek, M.; Humphry-Baker, R.; Viruela, R.; Orti, E.; Zakeeruddin, S.; Graetzel, M.; Delgado, J. L.; Martin, N. *Chem. Eur. J.* **2012**, *18*, 11621.

(13) Kocherzhenko, A. A.; Siebbeles, L. D. A.; Grozema, F. C. *J. Phys. Chem. Lett.* **2011**, *2*, 1753.

(14) (a) Diederich, F.; Faust, R.; Gramlich, V.; Seiler, P. *J. Chem. Soc., Chem. Commun.* **1994**, 2045. (b) Faust, R.; Diederich, F.; Gramlich, V.; Seiler, P. *Chem. Eur. J.* **1995**, *1*, 111. (c) Campbell, K.; McDonald, R.; Branda, N. R.; Tykwinski, R. R. *Org. Lett.* **2001**, *3*, 1045. (d) Siemsen, P.; Gubler, U.; Bosshard, C.; Gunter, P.; Diderich, F. *Chem. Eur. J.* **2001**, *7*, 1333. (e) Campbell, K.; McDonald, R.; Ferguson, M. J.; Tykwinski, R. R. *Organometallics* **2003**, *22*, 1353. (f) Bruce, M. I.; Zaitseva, N. N.; Low, P. J.; Skelton, B. W.; White, A. H. *J. Organomet. Chem.* **2006**, *691*, 4273. (g) Akita, M.; Tanaka, Y.; Naitoh, C.; Ozawa, T.; Hayashi, N.; Takeshita, M.; Inagaki, A.; Chung, M.-C. *Organometallics* **2006**, *25*, 5261.

(15) (a) Cao, Z.; Ren, T. *Organometallics* **2011**, *30*, 245. (b) Xi, B.; Liu, I. P. C.; Xu, G. L.; Choduri, M. M. R.; De Rosa, M. C.; Crutchley, R. J.; Ren, T. *J. Am. Chem. Soc.* **2011**, *38*, 15094.

(16) (a) Xu, G.-L.; Xi, B.; Updegraff, J. B.; Protasiewicz, J. D.; Ren, T. *Organometallics* **2006**, *25*, 5213. (b) Zhao, Y.; Zhou, N.; Slepkov, A. D.; Ciulei, S. C.; McDonald, R.; Hegmann, F. A.; Tykwinski, R. R. *Helv. Chim. Acta* **2007**, *90*, 909. (c) Shoji, T.; Ito, S.; Okujima, T.; Morita, N. *Eur. J. Org. Chem.* **2011**, 5134. (d) Zhao, Y.; Luu, T.; Bernard, G. M.; Tearum, T.; McDonald, R.; Wasylishen, R. E.; Tykwinski, R. R. *Can. J. Chem.* **2012**, *90*, 994. (e) Forrest, W. P.; Cao, Z.; Hassell, K. M.; Prentice, B. M.; Fanwick, P. E.; Ren, T. *Inorg. Chem.* **2012**, *51*, 3261. (f) Forrest, W. P.; Cao, Z.; Hambrick, H. R.; Prentice, B. M.; Fanwick, P. E.; Wagenknecht, P. S.; Ren, T. *Eur. J. Inorg. Chem.* **2012**, *34*, 5616.

(17) Corey, E. J.; Fuchs, L. *Tetrahedron Lett.* **1972**, 3769.

(18) (a) Pedersen, B.; Wagner, G.; Herrmann, R.; Scherer, W.; Meerholz, K.; Schmälzlin, E.; Bräuchle, C. *J. Organomet. Chem.* **1999**, *590*, 129. (b) Tsuboya, N.; Hamasaki, R.; Ito, M.; Mitsuishi, M.; Miyashita, T.; Yamamoto, Y. *J. Mater. Chem.* **2003**, *13*, 511.

(19) (a) Luo, S.-J.; Liu, Y.-H.; Liu, C.-M.; Liang, Y.-M.; Ma, Y.-X. *Synth. Commun.* **2000**, *30*, 1569. (b) Courtney, D.; McAdam, C. J.; Manning, A. R.; Müller-Bunz, H.; Ortin, Y.; Simpson, J. *J. Organomet. Chem.* **2012**, *705*, 7.

(20) (a) Anthony, J.; Boldi, A. M.; Rubin, Y.; Hobi, M.; Gramlich, V.; Knobler, C. B.; Seiler, P.; Diederich, F. *Helv. Chim. Acta* **1995**, *78*, 13. (b) Nierengarten, J.-F.; Gu, T.; Hadziioannou, G.; Tsamouras, D.; Krasnikov, V. *Helv. Chim. Acta* **2004**, *87*, 2948. (c) Chalifoux, W. A.; Tykwinski, R. R. *Chem. Rec.* **2006**, *6*, 169.

(21) Clément, S.; Guyard, L.; Knorr, M.; Villafañe, F.; Strohmann, C.; Kubicki, M. M. *Eur. J. Inorg. Chem.* **2007**, 5052.

(22) (a) Kende, A. S.; Smith, C. A. *J. Org. Chem.* **1988**, *53*, 2655. (b) Vollhardt, P. C.; Winn, L. S. *Tetrahedron Lett.* **1985**, *26*, 709. (c) Yaun, Z.; Stringer, G.; Jobe, I. R.; Kreller, D.; Scott, K.; Koch, L.; Taylor, N. J.; Marder, T. B. *J. Organomet. Chem.* **1993**, *452*, 115. (d) Chemin, D.; Linstrumelle, G. *Tetrahedron* **1994**, *50*, 5335. (e) Hirsch, A.; Vostrowsky, O. *Sci. Synth.* **2008**, *43*, 37.

(23) (a) Uenishi, J.; Matsui, K. *Tetrahedron Lett.* **2001**, *42*, 4353. (b) Uenishi, J.; Kawahama, R.; Yonemitsu, O. *J. Org. Chem.* **1998**, *63*, 8965. (c) Myers, A. G.; Goldberg, S. D. *Angew. Chem., Int. Ed.* **2000**, *39*, 2732.

(24) (a) Frei, M.; Aradhya, S. V.; Hybertsen, M. S.; Venkataraman, L. *J. Am. Chem. Soc.* **2012**, *134*, 4003. (b) González, M. T.; Díaz, A.; Leary, E.; García, R.; Herranz, M. A.; Rubio-Bollinger, G.; Martín, N.; Agraït, N. *J. Am. Chem. Soc.* **2013**, *135*, 5420. (c) Pera, G.; Martín, S.; Ballesteros, L. M.; Hope, A. J.; Low, P. J.; Nichols, R. J.; Cea, P. *Chem. Eur. J.* **2010**, *16*, 13398. (d) Marqués-González, S.; Yufit, D. S.; Howard, J. A. K.; Martín, S.; Osorio, H. M.; García-Suárez, V. M.; Nichols, R. J.; Higgins, S. J.; Cea, P.; Low, P. J. *Dalton Trans.* **2013**, *42*, 338.

(25) (a) McEwen, C. N.; McKay, R. G.; Larsen, B. S. *Anal. Chem.* **2005**, *77*, 7826. (b) Smith, M. J. P.; Cameron, N. R.; Mosely, J. A. *Analyst* **2012**, *137*, 4524.

(26) Baronetskii, A. O.; Kuz'yants, G. M. *Russ. Chem. Bull.* **1980**, *29*, 1267.

(27) Klamt, A.; Schüürmann, G. *J. Chem. Soc., Perkin Trans. 2* **1993**, *5*, 799.

(28) (a) Renz, M.; Theilacker, K.; Lambert, C.; Kaupp, M. *J. Am. Chem. Soc.* **2009**, *131*, 16292. (b) Kaupp, M.; Renz, M.; Parthey, M.; Stolte, M.; Würthner, F.; Lambert, C. *Phys. Chem. Chem. Phys.* **2011**, *13*, 16973. (c) Parthey, M.; Gluyas, J. B. G.; Schauer, P. A.; Yufit, D. S.; Howard, J. A. K.; Kaupp, M.; Low, P. J. *Chem. Eur. J.* **2013**, *19*, 9780.

(29) (a) Munzarová, M.; Kaupp, M. *J. Phys. Chem. A* **1999**, *103*, 9966. (b) Munzarová, M. L.; Kubácek, P.; Kaupp, M. *J. Am. Chem. Soc.* **2000**, *112*, 11900.

(30) Coulson, D. R. *Inorg. Synth.* **1972**, *13*, 121.

(31) Krejčík, M.; Daněk, M.; Hartl, F. *J. Electroanal. Chem.* **1991**, *317*, 179.

(32) Sheldrick, G. M. *Acta Crystallogr., Sect. A* **2008**, *64*, 112.

(33) Dolomanov, O. V.; Bourhis, L. J.; Gildea, R. J.; Howard, J. A. K.; Puschmann, H. *J. Appl. Crystallogr.* **2009**, *42*, 339.

(34) TURBOMOLE V6.4 2012, a development of University of Karlsruhe and Forschungszentrum Karlsruhe GmbH, 1989−2007, TURBOMOLE GmbH, since 2007.

(35) Renz, M.; Theilacker, K.; Lambert, C.; Kaupp, M. *J. Am. Chem. Soc.* **2009**, *131*, 16292.

(36) (a) Renz, M.; Theilacker, K.; Lambert, C.; Kaupp, M. *J. Am. Chem. Soc.* **2009**, *131*, 16292. (b) Kaupp, M.; Renz, M.; Parthey, M.; Stolte, M.; Würthner, F.; Lambert, C. *Phys. Chem. Chem. Phys.* **2011**, *13*, 16973. (c) Renz, M.; Kaupp, M. *J. Phys. Chem. A* **2012**, *116*, 10629. (d) Renz, M.; Kess, M.; Diedenhofen, M.; Klamt, A.; Kaupp, M. *J. Chem. Theory Comput.* **2012**, *8*, 4189. (e) Völker, S. F.; Renz, M.; Kaupp, M.; Lambert, C. *Chem. Eur. J.* **2011**, *17*, 14147.

(37) Klamt, A.; Schüürmann, G. *J. Chem. Soc., Perkin Trans. 2* **1993**, *5*, 799.

(38) (a) Schäfer, A.; Horn, H.; Ahlrichs, R. *J. Chem. Phys.* **1992**, *97*, 2571. (b) Weigend, F.; Ahlrichs, R. *Phys. Chem. Chem. Phys.* **2005**, *7*, 3297.

(39) (a) Scott, A. P.; Radom, L. *J. Phys. Chem.* **1996**, *100*, 16502. (b) Roder, J. C.; Meyer, F.; Hyla-Kryspin, I.; Winter, R. F.; Kaifer, E. *Chem. Eur. J.* **2003**, *9*, 2636.

(40) Varetto, U. *MOLEKEL 5.4*; Swiss National Supercomputing Centre, Manno, Switzerland.